



Perturbation Solutions for the Study of MHD Blood as a Third Grade Nanofluid Transporting Gold Nanoparticles through a Porous Channel

Akinbowale T. Akinshilo, Gbeminiyi M. Sobamowo

Department of Mechanical Engineering, University of Lagos, Akoka, Yaba, Lagos, Nigeria

Received January 05 2017; revised February 10 2017; accepted for publication March 15 2017.
Corresponding author: A.T. Akinshilo, ta.akinshilo@gmail.com

Abstract

In this paper, the flow, thermal and concentration analyses of blood as a third grade with gold as nanoparticles through a porous channel are carried out using regular perturbation method. The analysis are carried out using Vogel's model of temperature-dependent viscosity. The developed models were used to investigate the effects of the nano particles on the concentration, temperature and velocity of the fluid as it flows through the porous medium of a hollow channel in the presence of magnetic field. Also, the effects of fluid parameters such as Brownian motion, thermophoresis, viscous dissipation, non-Newtonian, porosity, magnetohydrodynamics (MHD), diffusion constant at various values on the fluid were established. The results generated in this work were found to be in good agreement with the results found in literature.

Keywords: Perturbation solutions; Magnetohydrodynamics; Blood; Third grade; Nanofluid.

1. Introduction

The study of blood flow as proven to be an area of increasing research interest especially in biomedical science and engineering. In order to properly analyze the flow, blood is considered as a third grade fluid and gold particles are used as nanoparticles. The relevance of study in biomedical science and engineering cannot be over-emphasized as it better encapsulate therapeutic molecules leading to efficient drug transport during disease treatment. Under such flow and during treatment, the effects of magnetic field on the flow of blood through a medium are analyzed. Xu and Liao [1] investigated the MHD flow of non-Newtonian fluid developed due to stretching plates where the effect of power law index on fluid velocity was presented while Kumar et al. [2] studied the effect of synthesizing gold nanoparticles with Ziniger officinale extract with the purpose of determining its compatibility with blood. Ogulu and Amos [3] analyzed the flow of blood through the blood vessels in the heart employing the Navier Stokes equation in the presence of magnetic field. Few years later, Ellahi et al. [4] presented the effects of (MHD) flow and heat transfer on non-Newtonian nanofluid flowing through a porous coaxial cylinder under slip boundary conditions. Baoku et al. [5] studied the effects of heat and mass transfer on an MHD third grade fluid flowing under partial slip past a porous plate while analytical solutions of MHD non Newtonian fluid flowing through a pipe with temperature dependent model of viscosity was presented by Ellahi [6] using the homotopy analysis method (HAM). Shaoqin and Huoyuan [7] analyzed incompressible MHD equations using the least square method. Also, Hatami et al. [8] investigated the effect of nanoparticles on non-Newtonian third grade nanofluid exposed to magnetic field where they discovered that the present of nanoparticles leads to decrease in the velocity fields. In this work, regular perturbation method is used to develop approximate analytical solutions for the flow, thermal and concentration analysis of blood as a third grade nanofluid under the influence of magnetic field. The developed models are used to investigate the effects of the nano particles on the concentration, temperature and velocity of the fluid as it flows through the porous medium of a hollow channel in the presence of magnetic field. Also, the effects of fluid parameters such as Brownian motion, thermophoresis, viscous dissipation, non-Newtonian, porosity,

2. Model Development and Analytical Solution

Stress Tensor for the Third Grade Fluid is given by

$$T = -\rho I + \mu A_1 + \alpha_1 A_2 + \alpha_1 A_1^2 + S \quad (1-a)$$

where

$$S = \beta_1 A_3 + \beta_2 (A_1 A_2 + A_2 A_1) + \beta_3 (tr A_1^2) A_1 \quad (1-b)$$

In the equation three above T is the stress tensor, ρ is the pressure, I is the identity tensor, μ is the dynamic viscosity and $\alpha = (I = 1, 2)$, $\beta_i (1, 2, 3)$ are material constants. The A_n are Rivlin- Ericken tensor defined through

$$A_n = \frac{d}{dt} A_{n-1} + A_{n-1} L + L^T A_{n-1} \quad \text{for } n > 1 \quad (2)$$

where v denotes velocity field, grad is the operator gradient and d/dt is the material time derivative. When the motions of the fluid are thermodynamically compatible and it is assumed that the free energy is minimum when the fluid is locally at rest, then

$$\beta_1 = \beta_2 = 0, \quad \beta_3 \geq 0, \mu \geq 0, \quad \alpha_1 \geq 0 \quad [\alpha_1 + \alpha_2] \leq \sqrt{24\mu\beta_3} \quad (3)$$

Since $\beta_3 > 0$ the stress tensor can predict shear thickening as well as the normal stress. Thus stress tensor relation can be written as

$$T = -\rho I + \mu A_1 + \alpha_1 A_2 + \alpha_1 A_1^2 + [\mu + \beta_3 (tr A_1^2) A_1] \quad (4)$$

where velocity and temperature field can be expressed as

$$V = v(r), \quad \theta = \theta(r) \quad (5)$$

For steady incompressible, non-Newtonian nanofluid in the presence of magnetic field and hollow channel where the base fluid density is same as nanofluid is given as

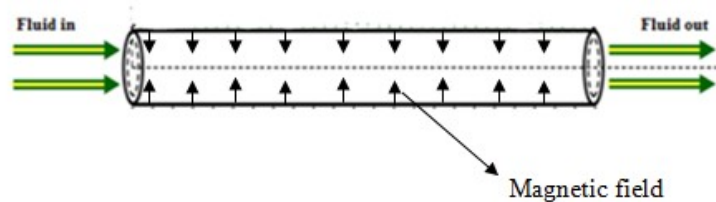


Fig. 1. Schematic diagram for the flow of blood as third grade nanofluid through a porous pipe under the influence of magnetic field

$$\rho = \phi \rho_p + (1 - \phi) [\rho_f (1 - \beta_T (\theta - \theta_w))] \quad (6)$$

The momentum conservation, mass, thermal energy and nanoparticles equations are given as

$$\rho_f \left(\frac{dV}{dt} + V \nabla V \right) = \text{div} T - \frac{\mu \phi}{k} \left(1 + \lambda_T \frac{\partial}{\partial t} \right) V + [\phi \rho_p + (1 - \phi) \rho_f [1 - \beta_T (\theta - \theta_w)]] g + J \times B \quad (7)$$

$$(\rho C)_f \left(\frac{d\theta}{dt} + V \nabla \theta \right) = k \nabla^2 \theta + (\rho C)_p \left[D_b \nabla \phi \cdot \nabla \theta + \frac{D_T}{\theta_w} \nabla \theta \cdot \nabla \theta \right] \quad (8)$$

$$\left(\frac{d\phi}{dt} + V \nabla \phi \right) = D_b \nabla^2 \phi + \frac{D_T}{\theta_w} \nabla^2 \theta \quad (9)$$

Since fluid is electrically conducting, for small Reynolds number induced magnetic field is neglected which gives

$$J \times B = -\sigma B_0^2 V \tag{10}$$

Using the boundary conditions

$$v(r) = 0, \quad \theta(r) = 0, \quad \phi(r) = 0, \quad \text{at } r = R \tag{11-a}$$

$$\frac{dv}{dr} = 0 = \frac{d\theta}{dr} = 0 = \frac{d\phi}{dr} = 0 \quad \text{at } r = 0 \tag{11-b}$$

Using the modified constitutive relation Eq. (4) in the balance of linear momentum, absence of body forces and assuming fluid can only undergo isochoric motion (i.e. $\text{div } v=0$). Upon dropping the bars for the sake of simplicity, the velocity, temperature and concentration profiles are given as [8]

$$\frac{d\mu}{dr} \frac{dv}{dr} + \frac{\mu}{r} \left(\frac{dv}{dr} + r \frac{d^2v}{dr^2} \right) + \frac{\Lambda}{r} \left(\frac{dv}{dr} \right)^2 \left(\frac{dv}{dr} + 3r \frac{d^2v}{dr^2} \right) = Pv + C + M^2v - Gr\theta - Br\phi \tag{12}$$

$$\alpha \frac{d^2\theta}{dr^2} + \frac{1}{r} \frac{d\theta}{dr} + \Gamma \left(\frac{dv}{dr} \right)^2 \left(\mu + \Lambda \left(\frac{dv}{dr} \right)^2 \right) + N_b \frac{d\theta}{dr} \frac{d\phi}{dr} + \alpha_1 N_t \left(\frac{d\theta}{dr} \right)^2 = 0 \tag{13}$$

$$N_b \left(\frac{d^2\theta}{dr^2} + \frac{1}{r} \frac{d\theta}{dr} \right) + N_t \left(\frac{d^2\phi}{dr^2} + \frac{1}{r} \frac{d\phi}{dr} \right) = 0 \tag{14}$$

Taking boundary condition under no slip condition as

$$v(r) = 0, \quad \theta(r) = 0, \quad \phi(r) = 0, \quad \text{at } r = 1 \tag{15-a}$$

$$\frac{dv}{dr} = 0 = \frac{d\theta}{dr} = 0 = \frac{d\phi}{dr} = 0 \quad \text{at } r = 0 \tag{15-b}$$

In this work, the Vogel’s model of viscosity is considered

$$\mu(T) = \mu_0 e^{(a/(b-T_0))} \quad \text{Vogel’s model} \tag{16}$$

Nondimensionalizing the Vogel’s viscosity model yields

$$\mu = e^{(A/(B-\theta)-T_0)} \tag{17}$$

With the aid of Maclaurins expansion, Vogel’s viscosity model can be written as

$$\mu = \exp\left(\frac{A}{B} - T_0\right) \left(1 - \frac{\epsilon A \theta}{B^2}\right) \tag{18}$$

Taking series solutions of velocity, temperature and concentration fields yields

$$v = v_0 + \epsilon v_1 + \epsilon^2 v_2 + O(\epsilon^3) \tag{19}$$

$$\theta = \epsilon \theta_1 + \epsilon^2 \theta_2 + O(\epsilon^3) \tag{20}$$

$$\phi = \epsilon \phi_1 + \epsilon^2 \phi_2 + O(\epsilon^3) \tag{21}$$

Decoupling Eq.12 into two parts, with the first part as

$$\frac{d\mu}{dr} \frac{dv}{dr} + \frac{\mu}{r} \left(\frac{dv}{dr} + r \frac{d^2v}{dr^2} \right) + \frac{\Lambda}{r} \left(\frac{dv}{dr} \right)^2 \left(\frac{dv}{dr} + 3r \frac{d^2v}{dr^2} \right) - C \tag{22}$$

While the Second part is as shown

$$Pv + M^2v - Gr\theta - Br\phi \tag{23}$$

Substituting Eqs. (18) and (19) into Eq. (22) yields

$$O(\epsilon^0): \quad \frac{1}{r} \frac{dv_0}{dr} + \frac{d^2v_0}{dr^2} = C \tag{24}$$

$$O(\epsilon^1): \frac{1}{r} \frac{dv_1}{dr} + \frac{d^2v_1}{dr^2} + \frac{\Lambda}{r} \left(\frac{dv_0}{dr} \right)^3 \frac{C^*}{C} + \frac{3\Lambda C}{C^*} \left(\frac{dv_0}{dr} \right)^2 \frac{d^2v_0}{dr^2} \tag{25}$$

$$O(\epsilon^2): \frac{-A}{B^2} \frac{d\theta_0}{dr} \frac{dv_0}{dr} + \frac{1}{r} \frac{dv_2}{dr} - \frac{1}{r} \frac{A}{B^2} \theta_0 \frac{dv_0}{dr} + \frac{d^2v_2}{dr^2} - \frac{A}{B^2} \theta_0 \frac{d^2v_0}{dr^2} + \frac{\Lambda C^*}{r C} \left(\frac{dv_0}{dr} \right)^2 \frac{dv_1}{dr} + 6 \frac{\Lambda C^*}{r C} \left(\frac{dv_0}{dr} \right) \frac{dv_1}{dr} \frac{dv_2}{dr} \tag{26}$$

Leading order boundary condition

$$v_0(1) = \theta_0(1) = \phi_0 = 0 = \frac{dv_0}{dr}(0) = \frac{d\theta_0}{dr}(0) = \frac{d\phi_0}{dr} = 0 \tag{27}$$

Integrating Eq. 24 twice and applying leading order boundary condition yields

$$v_0 = \frac{-C}{4} (1-r^2) \tag{28}$$

First order boundary condition

$$v_1(1) = \theta_1(1) = \phi_1 = 0 = \frac{dv_1}{dr}(0) = \frac{d\theta_1}{dr}(0) = \frac{d\phi_1}{dr} = 0 \tag{29}$$

Integrating Eq. 25 twice and applying the first order boundary condition yields

$$v_1 = -\frac{\Lambda C^4}{128} (1-r^4) + \frac{3\Lambda C^4}{128} (1-r^4) \tag{30}$$

Substituting Eqs. (18) – (21) into Eq. (13) yields

$$O(\epsilon^0): \alpha \frac{d^2\theta_0}{dr^2} + \frac{1}{r} \frac{d\theta_0}{dr} + 2 \frac{\Lambda C^*}{r C} \frac{dv_0}{dr} \frac{dv_1}{dr} + 2\Gamma\Lambda \left(\frac{dv_0}{dr} \right)^3 \frac{dv_1}{dr} \tag{31}$$

$$O(\epsilon): \alpha \frac{d^2\theta_1}{dr^2} + \frac{1}{r} \frac{d\theta_1}{dr} + 6\Gamma \frac{C^*}{C} \frac{dv_0}{dr} \frac{dv_1}{dr} + \Gamma \frac{C^*}{C} \left(\frac{dv_1}{dr} \right)^2 + 6\Gamma\Lambda \left(\frac{dv_0}{dr} \right)^2 \left(\frac{dv_1}{dr} \right)^2 + N_b \frac{d\theta_0}{dr} \frac{d\phi_0}{dr} + \alpha_1 N_t \left(\frac{d\theta_1}{dr} \right)^2 \tag{32}$$

Integrating Eq. (31) twice and applying the leading boundary condition Eq. (27) yields

$$\theta_0 = \frac{\Lambda\Gamma C^4(1-r^6)}{288} + \frac{\Lambda^2 C^7 \Gamma(1-r^8)}{4096} \tag{33}$$

Second order boundary condition

$$v_2(1) = \frac{dv_2}{dr}(0) = 0 \tag{34}$$

Integrating Eq. (26) twice and applying the second order boundary condition (29) yields

$$v_2 = \frac{\Lambda\Gamma C^5(1-r^8)}{3072B^2} - \frac{A\Lambda^2\Gamma C^8(1-r^8)}{17800\alpha B^2} - \frac{A\Lambda\Gamma C^5(16r^2-r^8)}{36864B^2} - \frac{A\Lambda^2\Gamma C^5(25r^2-r^{10})}{819200B^2} - \frac{\Lambda^2 C^6(1-r^5)}{400C^{*2}} - \frac{\Lambda^2 C^7(1-r^6)}{144C^{*2}} \tag{35}$$

Substituting Eq. (20) and (21) into Eq. (14) yields

$$O(\epsilon^1): N_b \frac{d^2\theta_0}{dr^2} + \frac{N_b}{r} \frac{d\theta_0}{dr} + N_t \frac{d^2\phi_0}{dr^2} + \frac{N_t}{r} \frac{d\phi_0}{dr} \tag{36}$$

$$O(\epsilon^2): N_b \frac{d^2\theta_1}{dr^2} + \frac{N_b}{r} \frac{d\theta_1}{dr} + N_t \frac{d^2\phi_1}{dr^2} + \frac{N_t}{r} \frac{d\phi_1}{dr} \tag{37}$$

Integrating Eq. (36) twice and applying the leading order boundary condition Eq. (27)

$$\phi_0 = \frac{N_b \Lambda C^4 \Gamma(1-r^6)}{288\alpha N_t} + \frac{N_b \Lambda^2 C^7 \Gamma(1-r^8)}{1024N_t} \tag{38}$$

Integrating Eq. (32) twice and applying the first order boundary condition Eq. (29) yields

$$\begin{aligned} \theta_1 = & \frac{\Lambda \Gamma C^5 (25r^4 - 4r^{10} - 84)}{460800B^2} - \frac{A \Lambda^2 \Gamma^2 C^8 (9r^4 - r^{12} - 8)}{235929B^2 \alpha} + \frac{\Gamma \Lambda^2 C^7 (1-r^8)}{4096\alpha C^*} \\ & + \frac{3\Gamma \Lambda^2 C^{10} (1-r^{10})}{12800\alpha C^*{}^2} - \frac{\Lambda^2 \Gamma^2 C^9 N_b^2 (15r^9 - 81r^{15} + 99)}{44789760\alpha^3 N_t} - \frac{\Lambda^4 \Gamma^2 N_b^2 C^{14} (289r^9 - 81r^{17} - 208)}{3068264448} \\ & + \frac{\Lambda^2 \Gamma^2 N_t C^9 \alpha_1 (1-r^{12})}{331776\alpha^3} + \frac{\Lambda^3 \Gamma^2 C^{11} N_t \alpha_1 (1-r^{14})}{602112\alpha^3} + \frac{\Lambda^4 \Gamma^2 C^{14} \alpha_1 N_t (1-r^{16})}{4194304\alpha} \\ & + \left(\frac{C^*}{C} + \Lambda \right) \cdot \left[\frac{A \Gamma^2 \Lambda C^6 (1-r^{10})}{38400\alpha^2 B^2} + \frac{A \Gamma^2 \Lambda^2 C^9 (1-r^{12})}{256320\alpha^2 B^2} \right. \\ & \left. + \frac{A \Lambda \Gamma^2 C^6 (25r^4 - r^{12} - 44)}{460800B^2 \alpha} + \frac{\Gamma \Lambda^2 C^7 (1-r^6)}{2880\alpha C^*{}^2} + \frac{\Gamma \Lambda^2 C^8 (1-r^8)}{1536\alpha C^*{}^2} \right] \end{aligned} \tag{39}$$

Integrating Eq. (37) twice and applying the first order boundary condition Eq. (29) yields

$$\begin{aligned} \phi_1 = & \frac{N_b A \Gamma C^5 (25r^4 - 16r^{10})}{460800\alpha B^2 N_t} - \frac{N_b A \Gamma^2 C^8 (9r^4 - r^{12})}{235929\alpha B^2 N_t} + \frac{\Gamma \Lambda^2 C^7 r^8}{4096\alpha C^* N_t} + \frac{3\Gamma \Lambda^3 C^{10} N_b r^{10}}{12800\alpha C^*{}^2 N_t} \\ & + \frac{N_b^3 \Gamma^2 \Lambda^4 C^{14} (256r^9 - 81r^6)}{2717908992} + \frac{\Lambda^2 \Gamma^2 N_b C^9 \alpha_1 r^{18}}{331776\alpha^3} + \frac{\Lambda^3 \Gamma^2 N_b C^{11} \alpha_1 r^{14}}{602112\alpha^3} + \frac{\Lambda^4 \Gamma^2 N_b C^{14} \alpha_1 r^{16}}{4194304\alpha^2} \\ & + \left(\frac{C^*}{C} + \Lambda \right) \cdot \left[\frac{N A \Gamma^2 \Lambda C^6 r^{10}}{38400\alpha^2 B^2 N_t} + \frac{N_b A \Gamma^2 \Lambda^2 C^9 r^{12}}{256320\alpha^2 B^2 N_t} + \frac{N_b A \Lambda \Gamma^2 C^9 (45r^4 - r^{12})}{11796480B^2 \alpha N_t} \right. \\ & \left. + \frac{N_b \Gamma \Lambda^2 C^7 r^6}{2880\alpha C^*{}^2 N_t} + \frac{N_b \Gamma \Lambda^2 C^8 r^8}{1536\alpha C^*{}^2 N_t} \right] \end{aligned} \tag{40}$$

Substituting Eq. (28), (29) and (30) into the series solution at the order of expansion finally give

$$\begin{aligned} v = & \frac{-C}{4} (1-r^2) - \frac{\Lambda C^4}{128} (1-r^4) + \frac{3\Lambda C^4}{128} (1-r^4) + \frac{\Lambda \Gamma C^5 (1-r^8)}{3072B^2} - \frac{A \Lambda^2 \Gamma C^8 (1-r^8)}{17800\alpha B^2} \\ & - \frac{A \Lambda \Gamma C^5 (16r^2 - r^8)}{36864B^2} - \frac{A \Lambda^2 \Gamma C^5 (25r^2 - r^{10})}{819200B^2} - \frac{\Lambda^2 C^6 (1-r^5)}{400C^*{}^2} - \frac{\Lambda^2 C^7 (1-r^6)}{144C^*{}^2} \end{aligned} \tag{41}$$

Coupling the velocity profile Eqs. (22) and (23) can be easily shown as

$$v - Pv - M^2 v + G_r \theta + B_r \phi = 0 \tag{42}$$

Substituting Eq. (33) and (39) into the series solution Eq. (20) finally give

$$\begin{aligned} \theta = & \frac{\Lambda \Gamma C^4 (1-r^6)}{288} + \frac{\Lambda^2 C^7 \Gamma (1-r^8)}{4096} + \frac{\Lambda \Gamma C^5 (25r^4 - 4r^{10} - 84)}{460800B^2} - \frac{A \Lambda^2 \Gamma^2 C^8 (9r^4 - r^{12} - 8)}{235929B^2 \alpha} + \frac{\Gamma \Lambda^2 C^7 (1-r^8)}{4096\alpha C^*} \\ & + \frac{3\Gamma \Lambda^2 C^{10} (1-r^{10})}{12800\alpha C^*{}^2} - \frac{\Lambda^2 \Gamma^2 C^9 N_b^2 (15r^9 - 81r^{15} + 99)}{44789760\alpha^3 N_t} - \frac{\Lambda^4 \Gamma^2 N_b^2 C^{14} (289r^9 - 81r^{17} - 208)}{3068264448} \\ & + \frac{\Lambda^2 \Gamma^2 N_t C^9 \alpha_1 (1-r^{12})}{331776\alpha^3} + \frac{\Lambda^3 \Gamma^2 C^{11} N_t \alpha_1 (1-r^{14})}{602112\alpha^3} + \frac{\Lambda^4 \Gamma^2 C^{14} \alpha_1 N_t (1-r^{16})}{4194304\alpha} \\ & + \left(\frac{C^*}{C} + \Lambda \right) \cdot \left[\frac{A \Gamma^2 \Lambda C^6 (1-r^{10})}{38400\alpha^2 B^2} + \frac{A \Gamma^2 \Lambda^2 C^9 (1-r^{12})}{256320\alpha^2 B^2} + \frac{A \Lambda \Gamma^2 C^6 (25r^4 - r^{12} - 44)}{460800B^2 \alpha} \right. \\ & \left. + \frac{\Gamma \Lambda^2 C^7 (1-r^6)}{2880\alpha C^*{}^2} + \frac{\Gamma \Lambda^2 C^8 (1-r^8)}{1536\alpha C^*{}^2} \right] \end{aligned} \tag{43}$$

Substituting Eqs. (38) and (40) into the series solution Eq. (21) finally gives

$$\phi = \frac{N_b \Lambda C^4 \Gamma (1-r^6)}{288 \alpha N_t} + \frac{N_b \Lambda^2 C^7 \Gamma (1-r^8)}{1024 N_t} + \frac{N_b A \Gamma C * C^5 (25r^4 - 16r^{10})}{460800 \alpha B^2 N_t} - \frac{N_b A \Gamma^2 C * C^8 (9r^4 - r^{12})}{235929 \alpha B^2 N_t} + \frac{\Gamma \Lambda^2 C^7 r^8}{4096 \alpha C * N_t} + \frac{3 \Gamma \Lambda^3 C^{10} N_b r^{10}}{12800 \alpha C *^2 N_t} + \frac{N_b^3 \Gamma^2 \Lambda^4 C^{14} (256r^9 - 81r^6)}{2717908992} + \frac{\Lambda^2 \Gamma^2 N_b C^9 \alpha_1 r^{18}}{331776 \alpha^3} + \frac{\Lambda^3 \Gamma^2 N_b C^{11} \alpha_1 r^{14}}{602112 \alpha^3} + \frac{\Lambda^4 \Gamma^2 N_b C^{14} \alpha_1 r^{16}}{4194304 \alpha^2} + \left(\frac{C *}{C} + \Lambda \right) \left[\frac{N A \Gamma^2 \Lambda C^6 r^{10}}{38400 \alpha^2 B^2 N_t} + \frac{N_b A \Gamma^2 \Lambda^2 C^9 r^{12}}{256320 \alpha^2 B^2 N_t} + \frac{N_b A \Lambda \Gamma^2 C^9 (45r^4 - r^{12})}{11796480 B^2 \alpha N_t} + \frac{N_b \Gamma \Lambda^2 C^7 r^6}{2880 \alpha C *^2 N_t} + \frac{N_b \Gamma \Lambda^2 C^8 r^8}{1536 \alpha C *^2 N_t} \right] \tag{44}$$

The velocity profile can be expressed in its final form by substituting values from Eqs. (43)- (45) as

$$(1-P-M^2) \left\{ \begin{aligned} & \left[\frac{-C}{4} (1-r^2) - \frac{\Lambda C^4}{128} (1-r^4) + \frac{3 \Lambda C^4}{128} (1-r^4) + \frac{\Lambda \Gamma C^5 (1-r^8)}{3072 B^2} - \frac{A \Lambda^2 \Gamma C^8 (1-r^8)}{17800 \alpha B^2} \right] \\ & \left[\frac{A \Lambda \Gamma C^5 (16r^2 - r^8)}{36864 B^2} - \frac{A \Lambda^2 \Gamma C^5 (25r^2 - r^{10})}{819200 B^2} - \frac{\Lambda^2 C^6 (1-r^5)}{400 C *^2} - \frac{\Lambda^2 C^7 (1-r^6)}{144 C *^2} \right] \end{aligned} \right\} \\ + Gr \left\{ \begin{aligned} & \left[\frac{\Lambda \Gamma C^4 (1-r^6)}{288} + \frac{\Lambda^2 C^7 \Gamma (1-r^8)}{4096} + \frac{\Lambda \Gamma C * C^5 (25r^4 - 4r^{10} - 84)}{460800 B^2} - \frac{A \Lambda^2 \Gamma^2 C * C^8 (9r^4 - r^{12} - 8)}{235929 B^2 \alpha} + \frac{\Gamma \Lambda^2 C^7 (1-r^8)}{4096 \alpha C *} \right. \\ & \left. + \frac{3 \Gamma \Lambda^2 C^{10} (1-r^{10})}{12800 \alpha C *^2} - \frac{\Lambda^2 \Gamma^2 C^9 N_b^2 (15r^9 - 81r^{15} + 99)}{44789760 \alpha^3 N_t} - \frac{\Lambda^4 \Gamma^2 N_b^2 C^{14} (289r^9 - 81r^{17} - 208)}{3068264448} + \right. \\ & \left. \frac{\Lambda^2 \Gamma^2 N_t C^9 \alpha_1 (1-r^{12})}{331776 \alpha^3} + \frac{\Lambda^3 \Gamma^2 C^{11} N_t \alpha_1 (1-r^{14})}{602112 \alpha^3} + \frac{\Lambda^4 \Gamma^2 C^{14} \alpha_1 N_t (1-r^{16})}{4194304 \alpha} + \left(\frac{C *}{C} + \Lambda \right) \right] \\ & \left[\frac{A \Gamma^2 \Lambda C^6 (1-r^{10})}{38400 \alpha^2 B^2} + \frac{A \Gamma^2 \Lambda^2 C^9 (1-r^{12})}{256320 \alpha^2 B^2} + \frac{A \Lambda \Gamma^2 C^6 (25r^4 - r^{12} - 44)}{460800 B^2 \alpha} + \frac{\Gamma \Lambda^2 C^7 (1-r^6)}{2880 \alpha C *^2} + \frac{\Gamma \Lambda^2 C^8 (1-r^8)}{1536 \alpha C *^2} \right] \end{aligned} \right\} \tag{45} \\ + Br \left\{ \begin{aligned} & \left[\frac{N_b \Lambda C^4 \Gamma (1-r^6)}{288 \alpha N_t} + \frac{N_b \Lambda^2 C^7 \Gamma (1-r^8)}{1024 N_t} + \frac{N_b A \Gamma C * C^5 (25r^4 - 16r^{10})}{460800 \alpha B^2 N_t} \right. \\ & \left. - \frac{N_b A \Gamma^2 C * C^8 (9r^4 - r^{12})}{235929 \alpha B^2 N_t} + \frac{\Gamma \Lambda^2 C^7 r^8}{4096 \alpha C * N_t} + \frac{3 \Gamma \Lambda^3 C^{10} N_b r^{10}}{12800 \alpha C *^2 N_t} + \frac{N_b^3 \Gamma^2 \Lambda^4 C^{14} (256r^9 - 81r^6)}{2717908992} \right. \\ & \left. + \frac{\Lambda^2 \Gamma^2 N_b C^9 \alpha_1 r^{18}}{331776 \alpha^3} + \frac{\Lambda^3 \Gamma^2 N_b C^{11} \alpha_1 r^{14}}{602112 \alpha^3} + \frac{\Lambda^4 \Gamma^2 N_b C^{14} \alpha_1 r^{16}}{4194304 \alpha^2} + \left(\frac{C *}{C} + \Lambda \right) \right] \\ & \left[\frac{N A \Gamma^2 \Lambda C^6 r^{10}}{38400 \alpha^2 B^2 N_t} + \frac{N_b A \Gamma^2 \Lambda^2 C^9 r^{12}}{256320 \alpha^2 B^2 N_t} + \frac{N_b A \Lambda \Gamma^2 C^9 (45r^4 - r^{12})}{11796480 B^2 \alpha N_t} + \frac{N_b \Gamma \Lambda^2 C^7 r^6}{2880 \alpha C *^2 N_t} + \frac{N_b \Gamma \Lambda^2 C^8 r^8}{1536 \alpha C *^2 N_t} \right] \end{aligned} \right\}$$

3. Results and Discussion

The results for the temperature, nanoparticles concentration and velocity profiles as generated from the developed models are shown in the Figures 1-14 b. Fig. 2 shows that as thermophoresis parameter (N_t) increases, temperature increases, while the Brownian motion parameter (N_b) increases with decrease in temperature distribution as shown in Fig.3. The nanoparticle concentration decrease when the brownian motion parameter (N_b) is increased which effect is significant near the walls as depicted in Fig. 4.

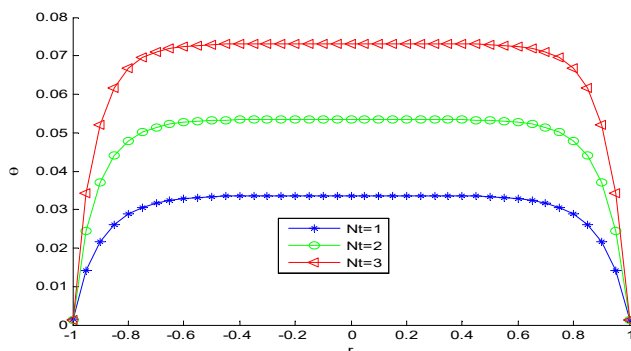


Fig. 2. Effect of thermophoresis parameter on the temperature distributions for when $-C = \Gamma = \Lambda = A = \alpha = N_b = \alpha_1 = B = T_0 = 1$.

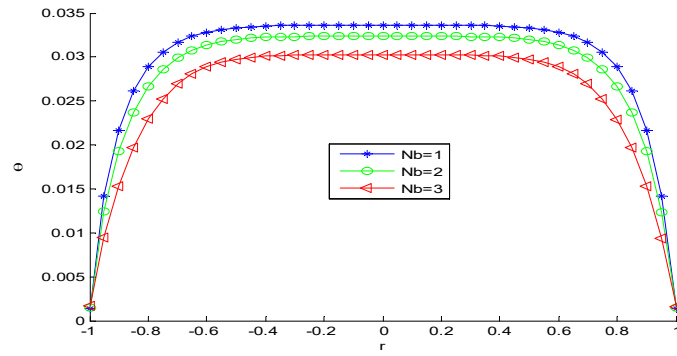


Fig. 3. Effect of varying Brownian motion parameter on the temperature distributions for when $-C = \Gamma = \Lambda = A = \alpha = N_t = \alpha_1 = B = T_0 = 1$.

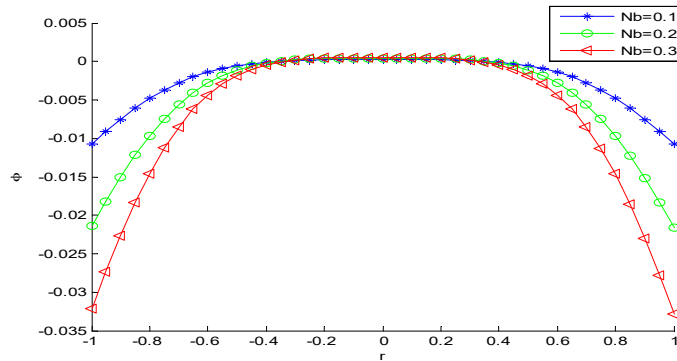


Fig. 4. Effect of varying Brownian motion parameter on the concentration for when $-C = \Gamma = \Lambda = A = \alpha = N_t = \alpha_1 = B = T_0 = 1$.

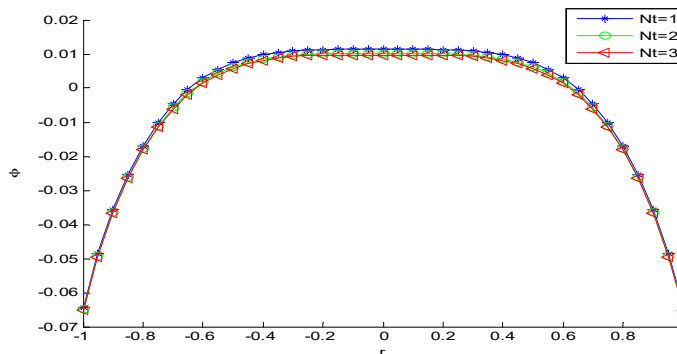


Fig. 5. Effect of varying thermophoresis parameter on the concentration for when $-C = \Gamma = \Lambda = A = \alpha = N_b = \alpha_1 = B = T_0 = 1$.

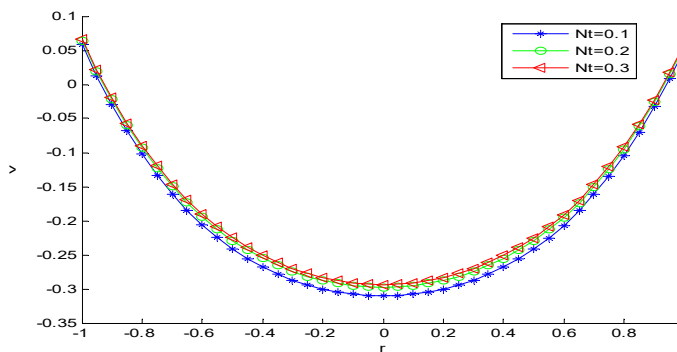


Fig. 6. Effect of varying thermophoresis parameter on the velocity distributions when $-C = \Gamma = \Lambda = A = \alpha = N_b = \alpha_1 = B = T_0 = P = M = Gr = Br = 1$.

The effect of thermophoresis parameter (N_t) on nanoparticles concentration as displayed in Fig. 5. An increase in the value of N_t , nanoparticles concentration decrease while the velocity profile increase slightly as shown in Fig. 6. At decreasing values of brownian motion parameter (N_b) as seen in Fig. 7, the velocity distribution decreases at the inner wall and increase at the outer wall. When the MHD parameter (M) is increased as depicted in Fig. 8. The velocity distribution decrease because increase in MHD parameter describes the strength of magnetic force field.

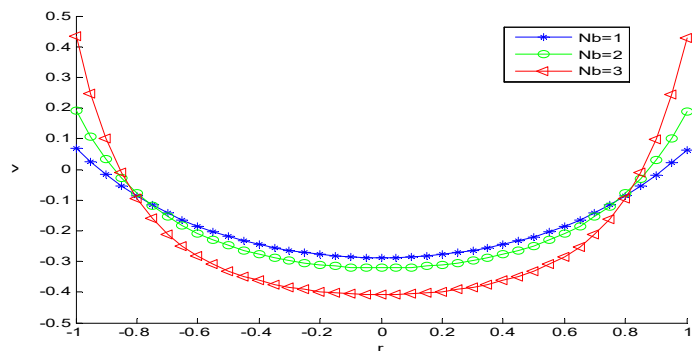


Fig. 7. Effect of varying Brownian motion parameter on the velocity distributions when $-C = \Gamma = \Lambda = A = \alpha = N_t = \alpha_1 = B = T_0 = P = M = Gr = Br = 1$.

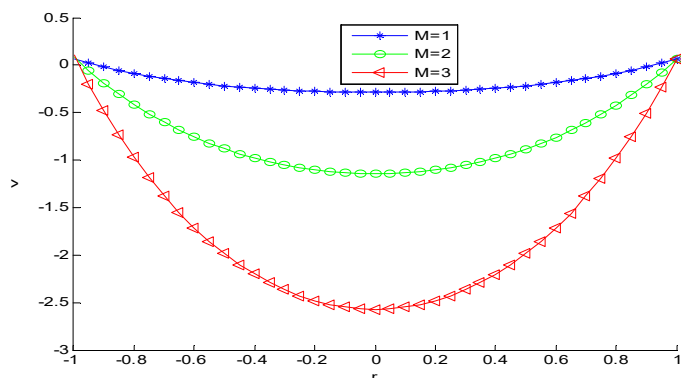


Fig. 8. Effect of varying MHD parameter on the velocity distributions when $-C = \Gamma = \Lambda = A = \alpha = N_b = \alpha_1 = B = T_0 = P = N_t = Gr = Br = 1$.

Fig. 9 shows that as viscous dissipation parameter (Γ) increases, the velocity distribution increases which effect is significant at the walls of the vessel and as we move near the center of the vessel it decreases rapidly. The effect of increasing values of the themophoretic diffusion constant (G_r) as shown in Fig. 10 confirms there is slight increase in velocity distribution. As pressure gradient value (C) becomes more negative as seen in the Fig. 11 velocity distribution decrease. Fig. 12 shows the effect of varying the Brownian diffusion constant (B_r), as seen from the plot at increasing values the velocity distribution decreases at the inner wall of the vessel while at the outer wall it increases. The non-Newtonian parameter (Λ) effect on the fluid flow is reported in Fig. 13 which shows at increasing values of Λ , velocity distribution decreases though the effect is very significant at the walls. Also Fig. 14 shows that increasing values of porosity parameter (P) gives a corresponding decrease in velocity distributions which effect is greatest towards the vessel center.

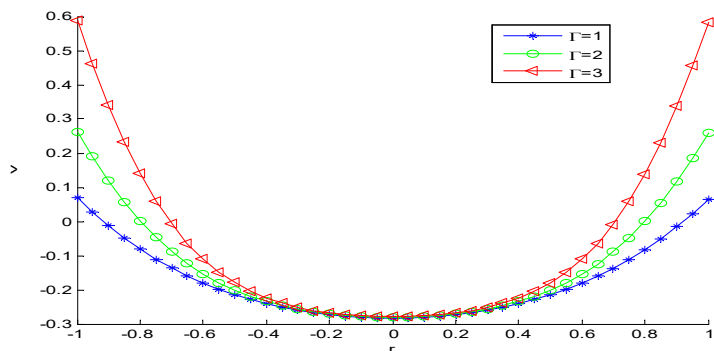


Fig. 9. Effect of varying viscous dissipation parameter on the velocity distributions when $-C = M = \Lambda = A = \alpha = N_b = \alpha_1 = B = T_0 = P = N_t = Gr = Br = 1$.

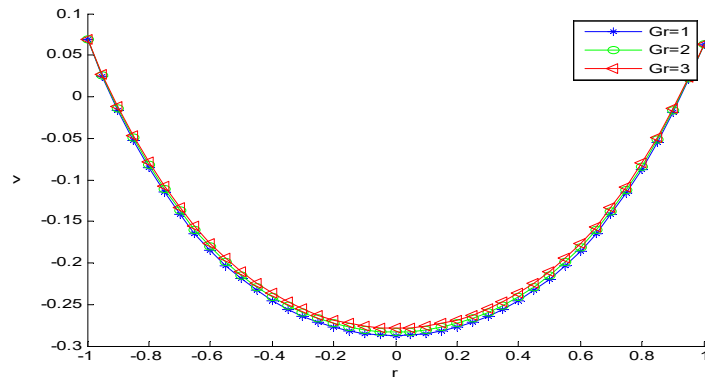


Fig. 10. Effect of varying thermophoresis diffusion constant on the velocity distributions when $-C = \Gamma = \Lambda = A = \alpha = N_b = \alpha_1 = B = T_0 = P = N_t = M = B_r = 1$.

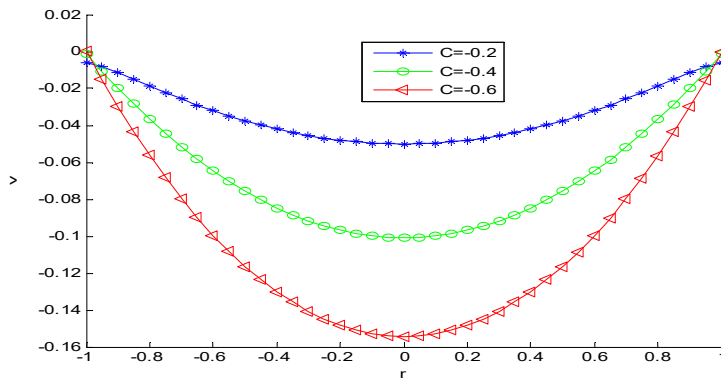


Fig. 11. Effect of varying pressure gradient parameter on the velocity distributions when $M = \Gamma = \Lambda = A = \alpha = N_b = \alpha_1 = B = T_0 = P = N_t = Gr = B_r = 1$.

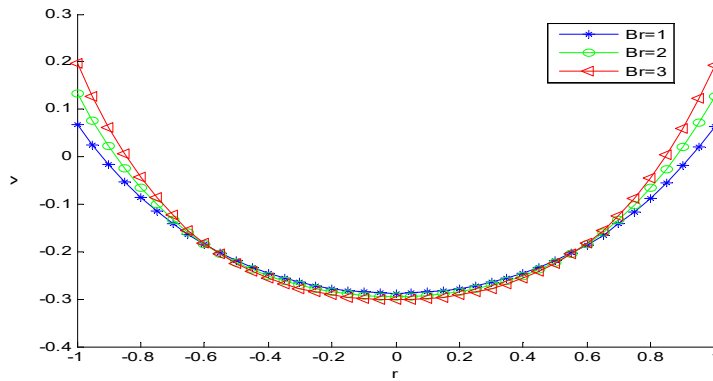


Fig. 12. Effect of varying Brownian diffusion constant on the velocity distributions when $-C = \Gamma = \Lambda = A = \alpha = N_b = \alpha_1 = B = T_0 = P = N_t = Gr = 1$.

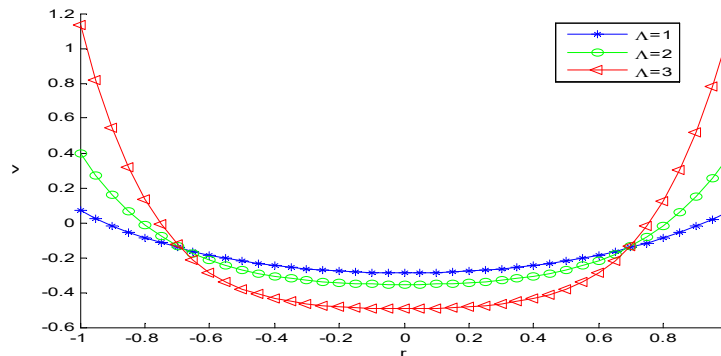


Fig. 13. Effect of varying Non Newtonian parameter on the velocity distributions when $-C = \Gamma = B_r = A = \alpha = N_b = \alpha_1 = B = T_0 = P = N_t = Gr = 1$.

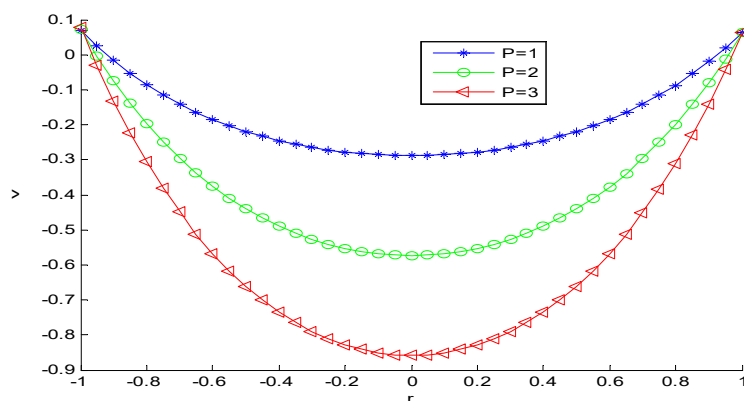


Fig. 14. Effect of varying porosity parameter on the velocity distributions when $-C = \Gamma = \Lambda = A = \alpha = N_b = \alpha_1 = B = T_0 = B_r = N_t = Gr = 1$.

4. Conclusion

In this work, approximate analytical solutions for the nonlinear analysis of heat transfer of MHD blood transporting gold nanoparticles in the presence of magnetic force fields in a porous channel has been analyzed using the regular perturbation method. The effects of various parameters such as Brownian diffusion constant, thermophoresis diffusion constant, viscous dissipation, MHD, porosity, Brownian motion and thermophoresis parameters at various values which show different fluid flow situations were established. The results can be used to further advance the study of blood transport in porous channel with nanoparticles which acts as an effective drug delivery mechanism in the treatment of blood related diseases.

Nomenclature

a and b	constant from dimensional Vogel’s viscosity model	μ	dimensionless viscosity
A	dimensionless constant from Vogel’s viscosity model	Γ	viscous heating parameter
B	dimensionless constant from Vogel’s viscosity model	θ	dimensionless temperature excess
C_0	Initial concentration of reacting species	Λ	non-Newtonian material parameter of the fluid
C	pressure gradient parameter	M	MHD parameter
$\partial P / \partial r$	pressure gradient along the normal to the pipe axis	D_b	Brownian diffusion coefficient
$\partial P / \partial Z$	pressure gradient in the axial direction	D_T	thermophoresis diffusion constant
$\partial P / \partial \phi$	pressure gradient in rotational direction	K	permeability
r	dimensional perpendicular distance in pipe axis	N_b	brownian motion parameter
R	radius of the pipe	N_t	thermophoresis parameter
T_0	initial temperature	P	porosity parameter
v(r)	dimensional velocity component in the z axis	ϕ	nanoparticle volume fraction
v	dimensionless velocity component in the z axis	G_r	thermophoresis diffusion constant
v_0	dimensional reference velocity	λ_T	retardation time
z	axis of the cylinder	β_T	volumetric expansion coefficient
α	material constant	ρ_f	density of base fluid
β	activation energy	ρ_p	density of nanoparticles
μ	dynamic shear viscosity	φ	porosity

References

[1] Xu, H., Liao, S. J. “Series solutions of unsteady magneto hydrodynamic flows of Non-Newtonian fluids caused by impulsive stretching plates,” *Journal of Non Newtonian fluid mechanics*, 147, pp. 46-55, 2005.

[2] Kumar, P. K., Paul, W., Sharma, C. P. “Green synthesis of gold nanoparticles with Zinigiberofficinaleextract,” *Process Biochemistry*, 46, pp. 2007-2013, 2011.

[3] Ogulu, A., Amos, E. “Modeling pulsatile blood flow within a homogeneous porous bed in the presence of a uniform magnetic field and time dependent suction,” *International communication of Heat Mass Transfer*, 34, pp.989-995, 2007.

[4] Ellahi, R., Zeeshan, A. Vafai, K., Rahman, H. U. “Series solutions for magneto hydrodynamic flow of non-Newtonian nanofluid and heat transfer in coaxial porous cylinder with slip condition,” *Proceedings of the Institution of Mechanical Engineering Part N*, 225, pp.123-132, 2011.

[5] Baoku, I. G., Olajuwon, B. I., A.O. Mustapha, “Heat and mass transfer on a MHD third grade fluid with partial

Journal of Applied and Computational Mechanics, Vol. 3, No. 2, (2017), 103-113

- slip flow past an infinite vertical insulated porous plate in a porous medium”, *International Journal Heat Fluid Flow*, 40, pp.81-88, 2013.
- [6] Ellahi, R., “The effect of MHD and temperature dependent viscosity on the flow of non-Newtonian nanofluid in a pipe, analytical solutions,” *Applied Mathematical model*, 37, pp.1451-1467, 2013.
- [7] Sheikholeslami, M. Hatamiand, M. Ganji, D. D. “Analytical investigation of MHD nanofluid in a semi porous channel, *Powder Technology*, 246, pp. 327-336, 2013.
- [8] Hatami, M., Hatami J., Ganji, D. D. “Computer simulation of MHD blood conveying gold nanoparticles as a third grade non-Newtonian nanofluid in a hollow porous vessel,” *Computer methods and programs in biomedicine*, 113, pp. 632-641, 2014.
- [9] Ogunmola, B. Y., Akinshilo, A. T., Sobamowo, M. G “Perturbation solutions for Hagen-Poiseuille flow and heat transfer of third grade fluid with temperature-dependent viscosities and internal heat generation,” *International Journal of Engineering Mathematics*, 2016, 8915745, 2016.
- [10] Fosdick, R. L., Rajagopal, K.R. “Thermodynamics and stability of fluids of third grade,” *Procter Society London*, Vol.339, pp.351-377, 1980.